ELSEVIER

Surface Science 401 (1998) 34–46

surface science

The reactions of diethylzinc on gallium-rich and arsenic-rich reconstructions of GaAs(100)

H.T. Lam [a], N. Venkateswaran [a], J.M. Vohs [a,*]

[a] *Department of Chemical Engineering, University of Pennsylvania, Pennsylvania, Philadelphia, PA 19104-6393, USA*

Received 13 January 1997; accepted for publication 14 November 1997

Abstract

Temperature programmed desorption (TPD) and high-resolution electron energy loss spectroscopy (HREELS) were used to investigate the reaction of diethylzinc (DEZ) on the Ga-rich (4×2) and As-rich (2×4) and $c(4\times4)$ reconstructions of GaAs(100). DEZ dissociatively adsorbed on all three surfaces to form ethyl groups and Zn atoms. The strength of Zn–surface interaction was found to be a function of surface As/Ga ratio. Adsorbed Zn atoms desorbed at 560 K on the Ga-rich (4×2) reconstruction and 585 K on the As-rich (2×4) reconstruction. For the $c(4\times4)$ surface, the primary Zn desorption feature was also at 585 K; however, additional Zn desorption features appeared between 600 and 700 K. In contrast to the interaction of Zn with GaAs(100), only minor variations in the reaction pathways for surface ethyl groups were observed as the surface As/Ga ratio was varied. The primary reaction pathway for ethyl groups on all three surfaces was b-hydride elimination at 570 K to produce ethylene. The ethylene yield was found to increase with increasing surface Ga concentration.

Keywords: Chemisorption; Electron energy loss spectroscopy; Gallium arsenide; Growth; Models of surface chemical reactions; Thermal desorption spectroscopy; Zinc selenide

1. Introduction

1.1. Background

The importance of surface processes in the growth of compound semiconductor thin films using metal organic chemical vapor deposition (MOCVD) has prompted numerous investigations of the mechanisms of the surface reactions of metal alkyls on GaAs(100) [1–9]. Even though the As-rich reconstructions of GaAs(100) are predominantly used as the growth surface in applications, with only a few exceptions [2,10–12], the majority of the surface reactivity studies have focused on reactions on Ga-rich surfaces [1–8]. Much less effort has been directed toward elucidating the mechanisms of the reactions of metal alkyls on As-rich GaAs(100) surfaces. As a result, the role of surface Ga and As atoms in the reaction of both alkyl groups and metal atoms on GaAs(100) is not well understood. We therefore report here the results of a temperature programmed desorption (TPD) and high-resolution electron energy loss spectroscopy (HREELS) study of the reaction of diethylzinc (DEZ) on the Ga-rich (4×2) and the As-rich (2×4) and $c(4\times4)$ reconstructions of GaAs(100).

In addition to providing a prototypical reactant for studying the influence of surface structure on

* Corresponding author. Fax: (+1) 215 573.2093; e-mail: vohs@cheme.seas.upenn.edu

0039-6028/98/$19.00
PII S0039-6028(97)00903-5

the reactions of metal alkyls on GaAs(100), our interest in DEZ also stems from the fact that it is used as a reactant in the MOCVD growth of ZnSe thin films [13,14]. The recent demonstration of ZnSe-based diode lasers that emit in the blue–green region of the spectrum [15] has renewed interest in developing efficient methods for ZnSe film growth. Due to the relatively small lattice mismatch ($\sim$0.27%) between ZnSe and GaAs, GaAs(100) is generally used as a substrate for ZnSe films. Studies of MBE-grown ZnSe–GaAs heterostructures have also shown that the electronic properties of the ZnSe–GaAs interface depend strongly on the GaAs(100) surface reconstruction during the initial stages of film growth [16–21]. An understanding of the reactions of both Zn and Se alkyls on GaAs(100) and the subsequent film nucleation processes may therefore be important in optimizing the growth of high-quality ZnSe–GaAs heterostructures using MOCVD.

1.2. Surface reconstructions of GaAs(100)

GaAs(100) exhibits a variety of atomic structures ranging from the As-rich c(4×4) reconstruction to the Ga-rich (4×2) reconstruction [22–29]. The formation of a specific surface structure depends largely on the preparation conditions and the ratio of Ga to As in the outermost atomic layer [30]. The local atomic structure of these surfaces has been studied both theoretically [22–26] and by a variety of experimental techniques [27–30] including scanning tunneling microscopy (STM) [31–40].

The most widely studied GaAs(100) surface is the As-rich (2×4) reconstruction. STM images [31,34,35] of this surface have demonstrated that it consists of As dimers arranged in groups of two or possibly three separated by a missing, dimer row. A schematic diagram of the proposed structure of this surface is displayed in Fig. 1a. The two As dimers, oriented along the [0$\bar{1}$1] direction, followed by a dimer vacancy form the (2×4) unit cell. It is also possible to have a configuration in which adjacent groups of As dimers are staggered in the [0$\bar{1}$1] direction. This results in a c(2×8) unit cell. It is likely that a real surface will consist of small domains of both the c(2×8) and (2×4) reconstructions [32]. In the remainder of this paper we will use (2×4) to denote the c(2×8)/(2×4) structure.

The Ga-rich (4×2) surface is generally thought to have a structure analogous to that of the (2×4) surface with the roles of Ga and As reversed [23,39]. A proposed structure for the (4×2) surface is displayed in Fig. 1b. As shown in this figure, the (4×2) surface is terminated with collections of Ga dimers separated by missing dimer rows. Note that a c(8×2) termination can also be formed by staggering the groups of Ga dimers. Ga-rich surfaces also sometimes exhibit a (4×1) LEED pattern [1,41]. It is thought that the (4×1) surface results from disorder within (4×2) domains [1]. In the remainder of this paper, we will use (4×2) to denote the c(8×2)/(4×2) structure.

The As-terminated c(4×4) reconstruction is formed for As coverages ranging from 0.86–1.75 ML [27,29,30,34]. Fig. 1c displays a model of the c(4×4) surface that has been proposed by Biegelsen et al. [34]. Note that this surface is terminated with 1.75 ML of As. The cross-sectional profile of the surface shows that in this reconstruction there are two As layers above the topmost Ga layer. Falta et al. have proposed a similar structure for this surface with the exception that a portion of the second layer As atoms are replaced with Ga [27].

2. Experimental

The experiments were performed in two separate ultra-high vacuum (UHV) surface analysis systems. One system was used primarily for TPD experiments and was equipped with a quadruple mass spectrometer (UTI) and a retarding field electron energy analyzer (Omicron) that was used for both low-energy electron diffraction (LEED) and Auger electron spectroscopy (AES). The second UHV system was used primarily for high-resolution electron energy loss spectroscopy (HREELS) and was equipped with an LK Technologies model 3000 HREEL spectrometer, a quadruple mass spectrometer (UTI) and LEED optics (OCI). Both UHV systems also contained a sputter ion gun for sample cleaning. A typical

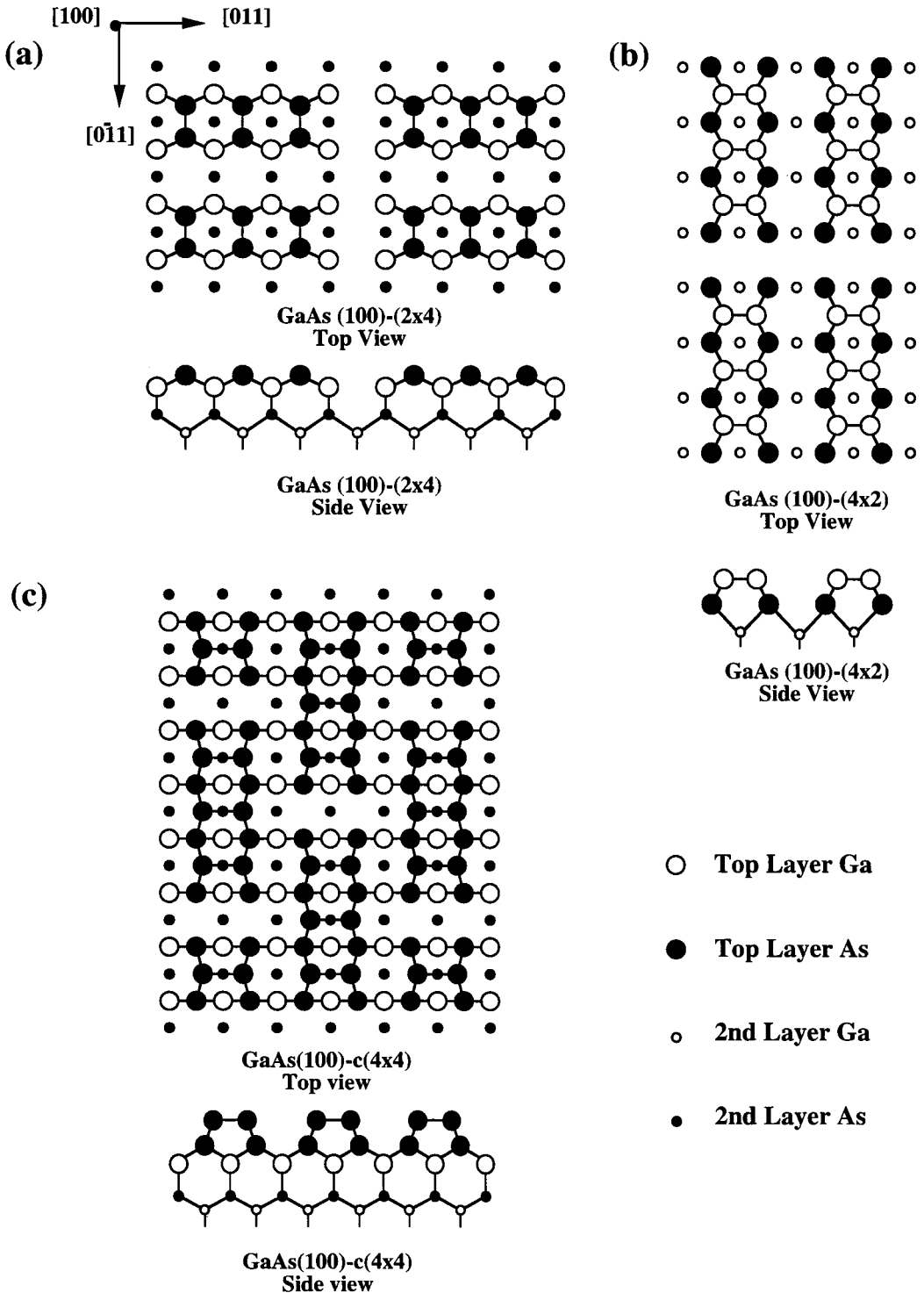

Fig. 1. Ball-and-stick models for three different surface reconstructions of GaAs(100): (a) As-rich (2×4) surface [31]; (b) Ga-rich (4×2) surface [39]; and (c) super As-rich surface [34].

working, base pressure of $\sim 3 \times 10^{-10}$ Torr was maintained in the UHV systems.

The GaAs samples were 0.8×1.2 cm in size and cut from a larger n-type GaAs(100) wafer (Te doped, $1–5 \times 1017$ atoms/cm3). Each sample was attached to a tantalum foil holder by welding with indium metal. The tantalum holder was, in turn, mounted on a UHV sample manipulator. Cooling of the sample to ~ 100 K was made possible by thermal contact with a liquid nitrogen reservoir. The sample temperature was monitored by a chromel–alumel thermal couple junction which was spot welded to the back of the tantalum foil holder. Heating the GaAs(100) sample was achieved by resistively heating the tantalum foil. A linear heating rate of 2.5 K/s was used in all TPD experiments. The mass spectrometer was computer multiplexed allowing multiple mass-to-charge ratios to be monitored during a single TPD run. Electronic grade DEZ obtained from Strem Chemicals was contained in a stainless steel cylinder and was purified by freeze–pump–thaw cycles prior to use. The DEZ was admitted into the vacuum chamber using a variable leak valve.

HREEL spectra were collected in the specular direction with a 5.0 eV electron beam incident 60° from the surface normal. During HREEL analysis the sample temperature was maintained at 100 K. The resolution of the HREEL spectra, as measured by the full-width at half maximum (FWHM) intensity of the elastic peak, was typically 4–5 meV. As in our previous studies, all HREEL spectra were subjected to a Fourier deconvolution procedure in order to remove phonon–phonon and phonon–adsorbate combination modes from the spectra and simplify the data analysis [42]. The application of this procedure to the HREEL spectra of GaAs(100) has been previously described in detail [41].

Once in vacuum the GaAs(100) surface was cleaned by sputtering with 0.5 keV Ar^+ ions for 30–40 min. While sputtering the temperature of the sample was maintained at 700 K. Immediately after sputtering, the sample was annealed for 4 min at 800 K. This produced a surface free from impurities which exhibited a LEED pattern characteristic of the Ga-rich (4×2) surface. The As-rich (2×4) and $c(4 \times 4)$ surfaces were prepared using the method described by Ludviksson et al. [43] which removes the top-most layer of Ga by etching with Cl_2.

A typical TPD spectrum obtained from a Cl_2-dosed GaAs(100)-(4×2) surface, which illustrates the etching of Ga by Cl_2, is displayed in Fig. 2. The spectra for mass-to-charge ratios (m/e) of 69, 75, 104 and 150 correspond to Ga^+, As^+, $GACl^+$, and As_2^+, respectively. $GaCl_2$ and $GaCl_3$ were monitored for but not detected. The Ga^+ signal tracks that of $GaCl^+$, indicating that it is due to the cracking of GaCl in the mass spectrometer ionizer. GaCl desorbs in a single first-order desorption feature centered at 620 K, whereas two separate As (both As and As_2) desorption features can be resolved at 670 and 730 K. These two arsenic desorption states are, respectively, labeled c and b (Fig. 2) after Banse and Creighton [11]. A continually increasing As desorption rate is observed for temperatures greater than 800 K. Both the peak shapes and the desorption temperatures for GaCl and As are in excellent agreement with those reported previously by Ludviksson et al. [43]. The As peaks are also in good agreement with those reported by Banse and Creighton [11]

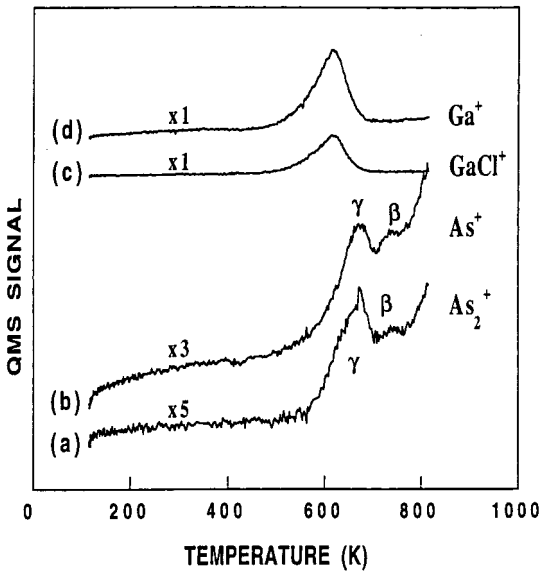

Fig. 2. TPD spectra for: (a) m/e 150 (As_2^+); (b) m/e 75 (As^+); (c) m/e 104 ($GaCl^+$); and (d) m/e 69 (Ga^+) obtained after saturating the Ga-rich (4×2) surface with Cl_2 at 100 K.

for the desorption of As from As-rich GaAs(100) surfaces.

To produce the c(4×4) reconstruction, the GaAs(100)-(4×2) surface was exposed to a saturation dose of Cl_2 and then annealed for 4 min at 620 K in order to desorb the surface Ga as GaCl. Surfaces prepared in this manner exhibited a two-fold symmetric LEED pattern characteristic of the c(4×4) As-rich reconstruction [30]. The (2×4) reconstruction was prepared by heating the sample to 680 K in order to desorb the c-As atoms. Formation of the (2×4) reconstruction was verified using LEED. Annealing an As-rich surface at 800 K was sufficient to revert it back to the Ga-rich (4×2) reconstruction.

3. Results

3.1. Temperature programmed desorption

The reaction of DEZ on GaAs(100) as a function of the surface reconstruction was initially studied using TPD. Since the reaction of DEZ on As-rich GaAs(100) surfaces has not been previously reported, the most extensive investigations were carried out for the c(4×4) surface. Fig. 3 displays TPD spectra for *m/e* 27, 29 and 64 obtained from DEZ-dosed GaAs(100)-c(4×4) as functions of the zinc alkyl exposure. Fig. 3c corresponds to the desorption spectra for *m/e* 64 (Zn^+). For DEZ exposures below 1.4 L, a single, broad *m/e* 64 peak is observed at 585 K. For exposures between 1 and 5 L, however, the *m/e* 64 desorption feature can be resolved into two overlapping peaks centered at 585 and 620 K. For exposures greater than 5 L, a third *m/e* 64 desorption feature appears as a shoulder (at 650 K) on the high-temperature side of the peak at 620 K. Mass-to-charge ratios of 93 and 122 corresponding to $ZnC_2H_5^+$ and $Zn(C_2H_5)_2^+$ ions, respectively, were also monitored for but not detected in this temperature range. This allows the *m/e* 64 peaks between 500 and 700 K to be assigned to Zn atoms rather than to a cracking fragment of DEZ. For DEZ exposures greater than 1.4 L, peaks for *m/e* 64, 93 and 122 were observed at 150 K and can be attributed to the desorption of molecularly adsorbed DEZ. The presence of multiple Zn peaks in the TPD spectra suggests that there is more than one adsorption site for Zn atoms on the c(4×4) surface.

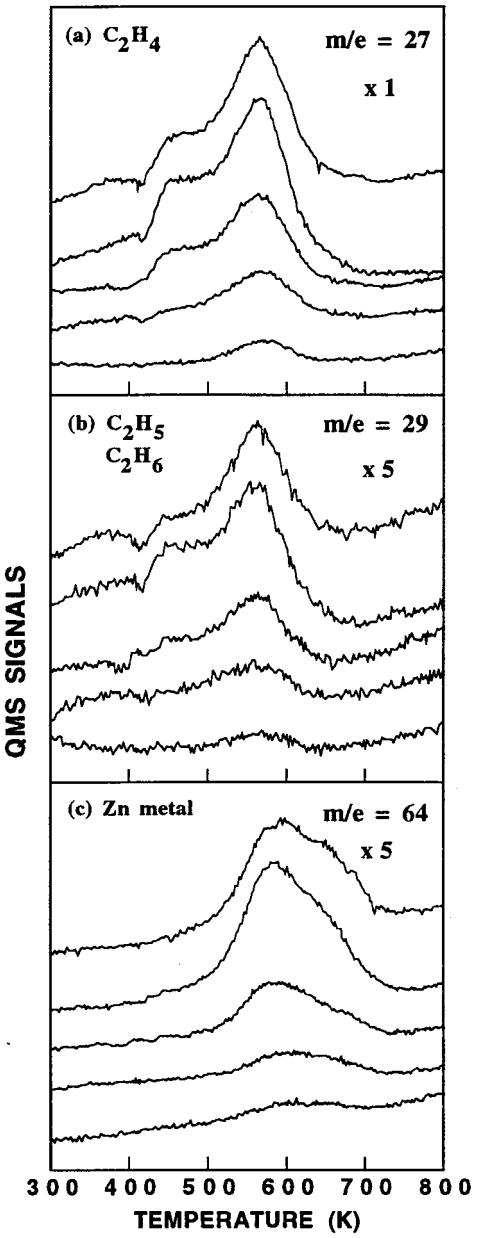

Fig. 3. TPD spectra for: (a) *m/e* 27 ($C_2H_3^+$); (b) *m/e* 29 ($C_2H_5^+$); and (c) *m/e* 64 (Zn^+) as a function of DEZ exposure at 100K. Estimated exposure levels for the curves shown are, from bottom to top, 0.7, 1.4, 3.0, 4.5 and 5.4 L.

In addition to Zn atoms, hydrocarbon species were also found to desorb during TPD of DEZ from the GaAs(100)-c(4×4) surface. Mass-to-charge ratios of 26 through 30 all exhibited peaks in the TPD spectra at temperatures between 420 and 700 K. The spectra obtained for *m/e* 27 and 29 are displayed in Fig. 3a and b, respectively. As mentioned above, zinc alkyl species were not detected in this temperature range, thus, these desorption features can be assigned primarily to hydrocarbons. The TPD spectra for *m/e* 26 and 27 exhibit a peak at 570 K for all DEZ exposures. A second smaller desorption feature for these *m/e* ratios appears at 460 K for exposures greater than 0.7 L. The TPD spectra for *m/e* 29 and 30 are similar to those for *m/e* 26 and 27 except that the maximum for the primary peak consistently appears at a slightly lower temperature of 560 K. A smaller feature at 460 K is also present in these spectra for high DEZ exposures.

The slight differences in the peak temperatures and the relative intensifies of the *m/e* 26 to 30 spectra indicate that more than one hydrocarbon species is produced between 420 and 700 K. The most intense peaks in the desorption spectra were *m/e* 26 and 27, which were of nearly equal intensity. This result is consistent with the majority of the hydrocarbon product being ethylene. The presence of significant intensity for *m/e* 29 is consistent with the desorption of ethyl radicals, while the signal for *m/e* 30 indicates that a small amount of ethane was also produced. For a 3.0 L DEZ exposure, the areas of the *m/e* 26, 29 and 30 peaks between 420 and 700 K relative to that of *m/e* 27 were 1.05, 0.17 and 0.16, respectively. Following the procedure of Ko et al. [51] and based on the relative peak areas and the cracking patterns [7,44] for ethane, ethylene and ethyl radicals, the relative product distribution was estimated to be 83% ethylene, 9% ethyl radicals and 8% ethane. The differences in peak temperatures are consistent with ethylene being produced at a slightly higher temperature than ethyl radicals or ethane. Using a standard Redhead analysis [45], the activation energy for ethylene production was estimated to be 151.2 kJ/mol.

A high background level of H_2 in the vacuum chamber used in this study necessitated that H_2 desorption spectra be collected at a lower mass spectrometer sensitivity setting than that used for the hydrocarbon and Zn desorption spectra. As a result it was not possible to collect H_2 spectra with a high signal-to-noise ratio. Several H_2 TPD experiments were performed, however, at a lower sensitivity in order to study H_2 production during TPD of the zinc alkyl-dosed surface. In these experiments it was found that H_2 desorbed coincidentally with ethylene at 570 K.

In addition to Zn metal, ethylene, ethyl radicals and ethane, for DEZ exposures greater than 3.0 L, a small amount of gallium alkyls were also detected during TPD from DEZ-dosed GaAs(100)-c(4×4). Curve (a) in Fig. 4 corresponds to the TPD spectrum for *m/e* 127 ($Ga(C_2H_5)_2^+$) obtained following exposure of the c(4×4) surface to 5.4 L of DEZ. The spectrum contains a peak centered at 440 K. Similar spectra were observed for *m/e* 69 (Ga^+) and 98 ($GaC_2H_5^+$). A peak was not detected in the spectrum for *m/e* 156 corresponding to the parent ion of triethylgallium (TEGa). The ratio of the intensity of *m/e* 156 to that of *m/e* 127 in the cracking pattern of TEGa [2,7], however, is less than 0.08 and thus a peak for *m/e* 156 may have gone undetected. We therefore collectively assign this product to TEGa. Note that the data in Fig. 4 were collected with a ten-fold higher mass spectrometer gain than that used while collecting

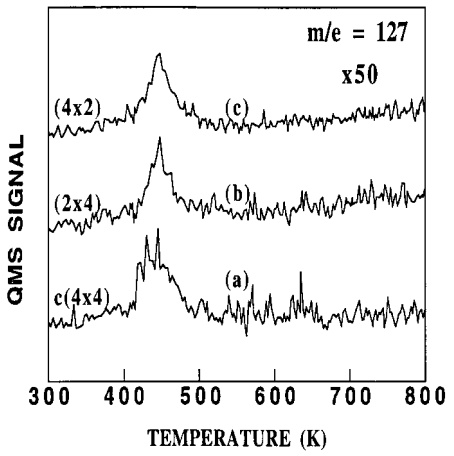

Fig. 4. Comparison of TPD spectra for *m/e* 127 ($Ga(C_2H_5)_2^+$) obtained from: (a) the c(4×4); (b) the (2×4); and (c) the (4×2) surfaces following a 3.0 L exposure of DEZ at 100 K.

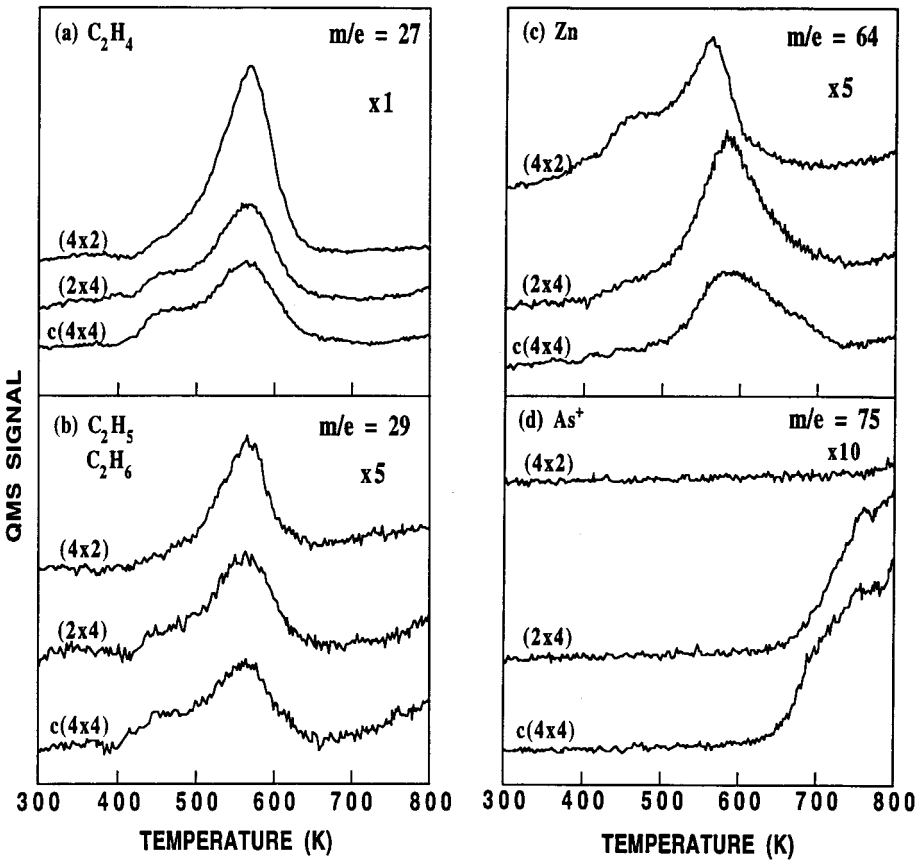

Fig. 5. Comparison of TPD spectra for: (a) *m/e* 27 ($C_2H_3^+$); (b) *m/e* 29 ($C_2H_5^+$); (c) *m/e* 64 (Zn^+); and (d) *m/e* 75 (As^+) obtained from the (4×2), (2×4) and $c(4\times4)$ surfaces dosed with 3.0 L of DEZ.

the data displayed in Figs. 2, 3 and 5. The total amount of TEGa produced was therefore quite small and contributed negligible intensity to the *m/e* 26, 27, 29 and 30 peaks near 460 K. Although the formation of arsenic alkyls was also monitored for during the TPD experiments, such products were not detected.

In order to assess how the surface reconstruction influences the reaction of DEZ on GaAs(100), TPD spectra were also collected for the Ga-rich (4×2) and As-rich (2×4) surfaces. A comparison of TPD spectra obtained from the three different reconstructions following a 3.0 L DEZ exposure is displayed in Fig. 5. As shown in this figure, decreasing the surface As coverage produced several changes in the TPD data. The most dramatic occurs in the spectra for atomic Zn desorption (*m/e* 64). On both the $c(4\times4)$ and (2×4) surfaces, the primary Zn desorption feature is centered at 585 K. The additional Zn desorption features, however, which appear between 600 and 700 K for the $c(4\times4)$ surface, are nearly absent for the (2×4) surface. In contrast to the As-rich surfaces, Zn desorption was found to occur at a significantly lower temperature on the Ga-rich (4×2) surface. For this surface, the Zn spectrum contains a large peak centered at 560 K and a smaller peak centered at 465 K. In our previous study of the reaction of DEZ on the Ga-rich (4×1) surface [41], it was found that the Zn peak at 465 K was only present for high DEZ coverages. Based on this observation and the fact that the activation energy for this peak is nearly identical to the heat of sublimation of Zn metal, it was concluded that it most probably

results from Zn desorption from Zn islands or clusters. The observed shift in Zn desorption temperature in going from the As-rich surfaces to the Ga-rich surface indicates that Zn interacts more strongly with surface As atoms than with surface Ga atoms. Using, a standard Redhead analysis [45] and assuming first-order kinetics and a pre-exponential factor of 10^{13}/s, the desorption activation energy for the primary Zn desorption peak is estimated to be 155 kJ/mol for the (2×4) and $c(4\times4)$ surfaces and 148 kJ/mol for the (4×2) surface.

Fig. 5a and b show that the desorption features for the hydrocarbon products are qualitatively similar for the three reconstructions. Note that the spectra reported here for the (4×2) reconstruction are in agreement with those obtained in our previous study of the reactivity of the Ga-rich (4×1) surface [41]. In all three cases, the primary peaks for *m/e* 26 and 27 are centered at 570 K, while those for *m/e* 29 and 30 are centered at 560 K. For the As-rich $c(4\times4)$ and (2×4) surfaces, the *m/e* 26, 27, 29 and 30 TPD spectra also contain a smaller peak centered at $\sim$460 K. This peak is absent in the spectra obtained from the Ga-rich (4×2) surface. The relative distribution of the various hydrocarbon products produced from each surface, as determined from the TPD results, are presented in Table 1. Note that the relative ethylene yield is higher on the (4×2) surface relative to the (2×4) and $c(4\times4)$ surfaces.

TPD spectra for *m/e* 75 (As^+) obtained from the zinc alkyl-dosed surfaces are displayed in Fig. 5d. As would be expected, arsenic or arsenic-containing products were not detected from the Ga-rich (4×2) surface. For the $c(4\times4)$ and (2×4) surfaces, the only As-containing products were As and As_2, which desorbed at temperatures greater than 650 K. Arsenic alkyls were not observed. As would be expected, the b-As peak was observed in the spectrum from the (2×4) surface, while both the b- and c-As peaks appear in the spectrum from the $c(4\times4)$ surface. The intensity of the c-peak relative to that of the b-peak is somewhat less, however, in the data from the DEZ-dosed $c(4\times4)$ surface relative to that in Fig. 2. Several possibilities exist to explain this difference. Note that the trailing edge of the Zn desorption feature overlaps with that of the c-As peak. It is therefore possible that adsorbed Zn atom suppress the intensity of the c-As desorption state. Since $c(4\times4)$ surfaces can exist for As coverages ranging from 0.86 to 1.75 ML [27,29,30,34], it is also possible that the Cl_2 etching procedure used to prepare the $c(4\times4)$ surface in this study results in As coverages toward the lower end of this range.

Table 1
Relative hydrocarbon product yields

	DEZ coverage (L)	Ethylene (%)	Ethyl radical (%)	Ethane (%)
$c(4\times4)$	5.4	83	9	8
(2×4)	5.4	81	11	8
(4×2)	3.0	91	6	3

TPD spectra for *m/e* 127 (TEGa) obtained from each GaAs(100) reconstruction following a 5.4 L DEZ exposure are displayed in Fig. 4. Note again that this set of TPD spectra was recorded at a higher mass spectrometer sensitivity (by a factor of 10) than that used for the data displayed in Figs. 2, 3 and 5. On each reconstruction the *m/e* 127 spectra contain a single peak centered at 440 K. One might expect that the amount of TEGa produced would decrease with increasing surface As-coverage. Surprisingly, this is not the case. The area of the *m/e* 127 peak is roughly the same on all three reconstructions and the amount of TEGa produced was always less than 1% of the total amount of ethylene produced.

3.2. HREELS

In order to identify stable surface intermediates involved in the reaction of DEZ on As-rich GaAs(100) surfaces, vibrational spectra of DEZ-dosed GaAs(100)-$c(4\times4)$ as a function of temperature were obtained using HREELS. Similar spectra for the Ga-rich GaAs(100)-(4×1) surface have been previously reported [46]. Fig. 6 displays deconvoluted HREEL spectra of DEZ-dosed GaAs(100)-$c(4\times4)$. Spectrum (a) in this figure corresponds to the clean $c(4\times4)$ surface. The peak near 600 cm^{-1} is an artifact due to incomplete removal of the first phonon combination peak by the deconvolution procedure. Although the loca-

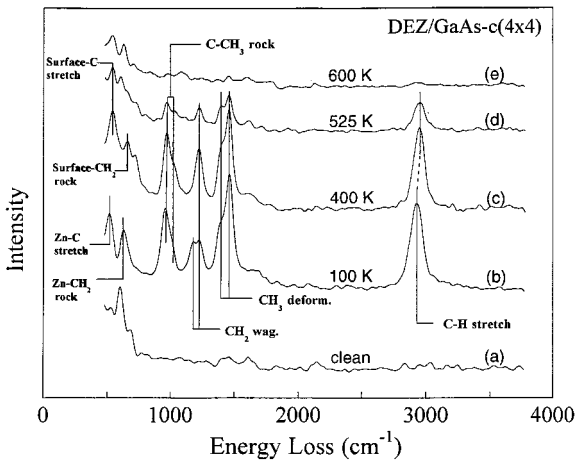

Fig. 6. Fourier deconvoluted HREEL spectra of: (a) the clean GaAs(100)-c(4×4) surface; and (b) the same surface dosed with 10 L of DEZ at 100 K, and after heating to (c) 400, (d) 525 and (c) 600 K.

tion of this peak remains fixed, its intensity varies somewhat from spectrum to spectrum and is generally less intense on adsorbate-covered surfaces. Spectrum (b) was obtained following a 10 L zinc alkyl exposure at 100 K. The remaining spectra were collected after briefly annealing the DEZ-dosed surface to a series of higher temperatures.

Based on the TPD results, following a 10 L DEZ exposure at 100 K, the c(4×4) surface is covered with multilayers of molecularly adsorbed DEZ. Thus, the peaks in this spectrum can be assigned by comparison with the IR and Raman spectra of vapor-phase [47] and liquid-phase [48] DEZ. The peaks centered between 900 and 3000 cm^{-1} are indicative of ethyl groups and can be assigned to CH_2 wagging modes (1180 and 1230 cm^{-1}), CH_3 deformation modes (1390 and 1460 cm^{-1}) and a C–H stretch (2930 cm^{-1}). Since in IR spectra the frequencies of C–CH_3 rocking and C–C stretching modes are similar [48], the peaks at 960 and 1015 cm^{-1} are collectively assigned to these modes. The peaks at 515 and 625 cm^{-1} can be assigned to a Zn–C stretching mode and a Zn–CH_2, rocking mode, respectively. This spectrum is similar to that reported previously for DEZ condensed on the (4×1) surface [46].

Except for a decrease in the intensity of the CH_2 wagging mode at 1180 cm^{-1}, heating the DEZ-dosed surface to 400 K in order to desorb the condensed multilayers produced little change in the peaks above 800 cm^{-1} which are characteristic of ethyl groups. More noticeable changes occurred, however, in the surface–C stretching region at low energy. Upon heating to 400 K, the metal–C stretch shifted from 515 to 540 cm^{-1}, whereas the metal–CH_2 rock shifted from 625 to 660 cm^{-1} and a new small peak is evident at 750 cm^{-1}. These changes can be attributed to dissociation of the adsorbed DEZ to form surface bound ethyl groups and Zn atoms. Since the metal–carbon stretching modes in molecular TEGa and TEAs have similar frequencies [49], a definitive assignment of the low-energy modes to ethyl groups adsorbed on either surface As or Ga atoms is not possible. On the As-rich c(4×4) surface, however, the ethyl groups are most probably coordinated to As atoms.

Further heating of the DEZ-dosed surface to 525 K resulted in a large decrease in the intensity of the adsorbate vibrational modes. This can be attributed to desorption of a portion of the ethyl groups and is consistent with the TPD results. The spectrum obtained after annealing at 600 K [spectrum (e)] is similar to that of the clean surface except that the deconvolution artifact is less intense. The absence of peaks above 800 cm^{-1} in this spectrum indicates that the reaction of DEZ on the c(4×4) surface does not result in the deposition of small hydrocarbon fragments on the surface. This result is consistent with that obtained for the reaction of DEZ on the (4×2) surface.

4. Discussion

Variations in the surface reconstruction were found to have a significant effect on the interaction of Zn atoms with the GaAs(100) surface. On the Ga-rich (4×2) surface the primary Zn desorption peak was centered at 560 K, while on the As-rich (2×4) and c(4×4) surfaces it was centered at 585 K. This result is similar to that obtained in our previous study of the interaction of DMZ with GaAs(100) [50]. On the (4×2) surface, Zn atoms most probably insert into the strained Ga–Ga dimer bonds forming a Zn species that bridges

between two surface Ga atoms. Note that since Zn has a valency of two, this adsorption site is consistent with the valence electron counting rules that are commonly used to predict the structure of GaAs surfaces [22]. In addition to the Zn peak at 560 K, on the (4×2) surface a smaller Zn desorption feature appears at 460 K. It has previously been shown that this low-temperature state becomes populated only once the peak at 560 K saturates [46]. The average activation energy for this low-temperature peak, as determined from the TPD data, is approximately 139 kJ/mol which is close to the heat of sublimation of Zn metal. Thus, this peak may result from desorption from Zn islands or clusters that form at high coverages once the Ga dimer sites have become populated.

The increase in the Zn desorption temperature from 560 to 585 K in going from the (4×2) to the (2×4) surface demonstrates that Zn atoms interact more strongly with As-rich surfaces than with Ga-rich surfaces. On the (2×4) surface, the most likely Zn adsorption site is across an As–As dimer. This adsorption site again obeys the valence electron counting rules. Since the $c(4\times4)$ surface is also terminated with As dimers, one would expect the interaction of Zn atoms with this surface to be similar to that with the (2×4) surface. As shown in Fig. 5, this is indeed the case. Both the (2×4) and $c(4\times4)$ surfaces have Zn desorption peaks at 585 K. Note, however, that there are additional Zn desorption features between 600 and 700 K on the $c(4\times4)$ surface. Thus, the interaction of Zn atoms with this surface is more complex than that with the (2×4) surface. One possible explanation for the multiple Zn peaks in the TPD data from the $c(4\times4)$ surface is that the As dimers on this surface do not all have equivalent chemical environments. As noted above, it has been proposed that the second atomic layer of this surface is composed of a mixture of both Ga and As atoms [27] as opposed to all As atoms [34]. Thus, the As dimer atoms may be coordinated to two arsenics, one arsenic and one gallium, or two galliums in the second atomic layer.

In contrast to the interaction of Zn atoms with GaAs(100), changes in the surface reconstruction produced only subtle differences in the chemistry of surface ethyl groups formed via dissociative adsorption of DEZ. On all three reconstructions the primary hydrocarbon product produced during TPD was ethylene, which desorbed at 570 K. The HREELS results obtained in this study for the $c(4\times4)$ surface and those reported previously for the (4×1) surface [46] demonstrate that the only stable adsorbed hydrocarbon species formed by reaction of DEZ on both Ga- and As-rich GaAs(100) surfaces are ethyl groups. Thus, the production of ethylene at 570 K is a reaction limited process involving abstraction of a b-hydrogen from adsorbed ethyl groups and the subsequent desorption of ethylene.

In addition to ethylene, a small fraction of the adsorbed ethyl groups reacted with surface hydrogen, formed during the b-hydride elimination reaction, to produce gaseous ethane at 560 K. It is interesting that the fractional yield of ethane was significantly lower on the Ga-rich (4×2) surface than on the As-rich (2×4) and $c(4\times4)$ surfaces. In previous studies of the reaction of alkyl groups on GaAs(100) produced by dissociative adsorption of both DMZ [41] and TEGa [2], it was found that the extent of dehydrogenation of surface alkyl groups increased with increasing surface Ga concentration. Based on this result it has been suggested that surface Ga atoms play an important role in hydride abstraction reactions from adsorbed alkyl groups on GaAs(100) [2]. Although the results of the present investigation are consistent with this conclusion, the fact that ethylene was still the predominant product on the As-rich $c(4\times4)$ surface suggests that As may also participate in hydride abstraction.

Previous work by Creighton [10] on the interaction of H atoms with GaAs(100)-(2×4) and GaAs(100)-(4×6) has shown that H atoms adsorbed on Ga sites desorb at $\sim$480 K, while those on As sites desorb at $\sim$660 K. This difference in the thermal stability of H atoms on Ga-rich and As-rich surfaces may also be an important factor in determining the ethane yield during the reaction of ethyl groups on GaAs(100). For the (2×4) and $c(4\times4)$ surfaces, b-hydride abstraction occurs at a temperature slightly below that of H_2 desorption, while for the (4×2) surface it occurs at a temperature slightly higher than that of H_2 desorption. Thus, the average hydrogen coverage

over the temperature range at which the b-hydride abstraction occurs would be higher on the As-rich surfaces relative to the Ga-rich surface. As a result, the reaction of adsorbed ethyl groups with H atoms to form ethane would be slightly favored on the As-rich surfaces.

Although the primary hydrocarbon desorption peaks occur at 570 K on both the As- and Ga-rich surfaces, the smaller hydrocarbon peaks at 460 K were only present on the As-rich surfaces. Since these smaller features occur at nearly the same temperature at which TEGa desorption was observed, they may be at least partially due to cracking fragments of TEGa. Note, however, that the relative intensity of the *m*/*e* 69 and 29 signals is such that the majority of the hydrocarbon product at 460 K cannot be assigned to TEGa desorption. It is also important to note that the relative intensifies of the low- and high-temperature peaks for *m*/*e* 26, 27, 29 and 30 did not vary significantly with coverage. The relative product yields for the low- and high-temperature features were also found to be nearly identical. Since the low-temperature peaks were observed only on the As-rich surfaces, it is tempting to assign them to a b-hydride elimination reaction involving surface As atoms and assign the higher temperature peaks to a b-hydride elimination reaction involving surface Ga atoms. The fact that the high-temperature peaks dominated on both the As- and Ga-rich surfaces is not completely consistent with this scenario, especially for the $c(4\times4)$ surface which is completely As terminated. The possibility that adsorbate-induced reconstructions result in Ga atoms being exposed on this surface cannot be ruled out, however.

It is interesting that on both Ga-rich and As-rich surfaces, gaseous ethylgallium species were produced during TPD of DEZ, while ethylarsenic species were not observed. The relative yield of TEGa was quite small on all three surfaces, with less than 1% of the adsorbed ethyl groups desorbing as TEGa. This result demonstrates that in the case of the Ga-rich (4×2) reconstruction, ethyl groups are not very effective in etching Ga atoms off the surface. For the As-rich surfaces, it is possible that the method of surface preparation (i.e. removal of the top most Ga layer as gallium chloride) results in a small number of Ga adatom defect sites. Interaction of ethyl groups with such sites may result in the production of TEGa during TPD.

It is useful to compare the results obtained in this study for the reaction of DEZ on GaAs(100) with those obtained in similar studies of the reaction of other ethyl-containing metal alkyl precursors such as TEGa [2,3,7], TEIn [8], TEAl [8] and TESb [52], on this substrate. A comparison of the results in the literature with those obtained here reveals that the interaction of all of the aforementioned metal alkyls with Ga-rich surfaces are similar. In all cases, the metal alkyls were found to adsorb dissociatively to form adsorbed metal atoms and ethyl groups. The primary reaction pathway for adsorbed ethyl groups was b-hydride elimination to produce ethylene at $\sim$565 K. As noted by Heitzinger et al. [8], this result indicates that the metal atom of the parent molecule does not participate in the hydride elimination reaction. In addition to DEZ, TEGa is the only other ethyl-containing metal alkyl for which reactivity studies have been carried out on both Ga-rich and As-rich GaAs(100) surfaces. Banse and Creighton [2] report that the primary reaction pathway for surface ethyl groups on TEGa-dosed (4×6) and (2×4) surfaces is also b-hydride elimination to form ethylene at 620 and 580 K, respectively. The results of that study as well as those reported here, thus, indicate that while changes in the surface As coverage may significantly influence the bonding of metal atoms to GaAs(100) surfaces, they produce only minor changes in the reactivity of ethyl groups on these surfaces.

5. Conclusions

The influence of surface structure on the reactions of DEZ on GaAs(100) was investigated by using TPD and HREELS. Diethylzinc was found to dissociatively adsorb on the Ga-rich (4×2) and the As-rich (2×4) and $c(4\times4)$ reconstructions of GaAs(100) to form surface ethyl groups and Zn atoms. The Zn desorption temperature was found to vary with the surface As coverage. In going from the Ga-rich (4×2) to the As-rich (2×4)

surface, the primary Zn desorption peak shifted from 560 to 585 K. This result indicates that Zn atoms interact more strongly with surface As dimers than with surface Ga dimers. For the As-rich c(4 × 4) surface, in addition to the primary Zn desorption feature at 585 K, Zn broad desorption features were also observed between 600 and 700 K during, TPD, suggesting that there are multiple absorption sites for Zn atoms on this surface. In contrast to the interaction of Zn with GaAs(100), the reaction pathways for ethyl groups on this surface were largely independent of the surface reconstruction. The primary reaction pathway for surface ethyl groups formed by dissociative adsorption of DEZ was b-hydride elimination to produce ethylene at 570 K and a small amount of ethane and ethyl radicals at 560 K. The relative yield of ethane to ethylene decreased slightly, however, with increasing surface As coverage. This difference most likely results from differences in the stability of H atoms adsorbed on surface Ga and As sites. The fact that b-hydride elimination was the primary reaction pathway on both As-rich and Ga-rich surfaces suggests that both surface Ga and As atoms can participate in hydride abstraction reactions. It was also found that the thermally induced reactions of ethyl groups on GaAs(100) do not result in carbon deposition.

Acknowledgements

We gratefully acknowledge the financial support of the National Science Foundation (Grant No. CTS-9321341) and the Laboratory for Research on the Structure of Matter at the University of Pennsylvania for the use of its facilities (NSF MRL Program, Grant No. DMR-9120668).

References

[1] J.R. Creighton, Surf. Sci. 234 (1990) 287.
[2] B.A. Banse, J.R. Creighton, Surf. Sci. 257 (1991) 221.
[3] A.J. Murrell, A.T.S. Wee, D.H. Fairbrother, N.K. Singh, J.S. Foord, G.J. Davies, D.A. Andrews, J. Appl. Phys. 68 (1990) 4053.
[4] E.T. Fitzgerald, C.L. French, N.K. Singh, J.S. Foord, J. Phys. Condens. Matter. 3 (1991) S173.
[5] M.E. Pemble, J.T. Allen, D.S. Buhaenko, S.M. Francis, P.A. Goulding, J. Lee, M.J. Parrott, Appl. Surf. Sci. 46 (1990) 32.
[6] J.A. McCaulley, R.J. Shui, V.M. Donnelly, J. Vac. Sci. Technol. A 9 (1991) 2872.
[7] V.M. Donnelly, J.A. McCaulley, Surf. Sci. 238 (1990) 34.
[8] J.M. Heitzinger, M.S. Jackson, J.G. Ekerdt, Appl. Phys. Lett. 66 (3) (1995) 352.
[9] M.C. Tamargo, J.L. deMiguel, D.M. Hwang, H.H. Farrell, J. Vac. Sci. Technol. B 6 (1988) 784.
[10] J.R. Creighton, J. Vac. Sci. Technol. A 8 (1990) 3984.
[11] B.A. Bansenauer, J.R. Creighton, Appl. Phys. Lett. 60 (1992) 856.
[12] H. Qi, P.E. Gee, R.F. Hicks, Surf. Sci. 347 (1996) 289.
[13] H. Ando, A. Taike, R. Kimura, M. Konagai, K. Takahashi, Jap. J. Appl. Phys. 25 (1986) L279.
[14] H. Ando, A. Taike, M. Konagai, K. Takahashi, Jap. J. Appl. Phys. 62 (1987) 1251.
[15] M.A. Haase, J. Qiu, J.M. DePuydt, H. Cheng, Appl. Phys. Lett. 59 (1991) 1272.
[16] J. Qiu, Q.D. Qian, R.L. Gunshor, M. Kobayashi, D.R. Menke, D. Li, N. Otsuka, Appl. Phys. Lett. 56 (1990) 1272.
[17] J. Qiu, D.R. Menke, M. Kobayashi, R.L. Gunshor, Q.D. Qian, D. Li, N. Otsuka, J. Crystal Growth 111 (1991) 747.
[18] S. Akram, H. Ehsani, L.B. Bhat, J. Crystal Growth 124 (1992) 628.
[19] Y. Wu, Y. Kawakami, S. Fujita, J. Crystal Growth 101 (1990) 78.
[20] M.C. Tamargo, J.L. deMiguel, D.M. Hwang, H.H. Farrell, J. Vac. Sci. Technol. B 6 (1988) 784.
[21] G. Bratina, R. Nicolini, L. Sorba, L. Vanzetti, G. Mula, X. Yu, A. Franciosi, J. Crystal Growth 127 (1993) 387.
[22] M.D. Pashley, Phys. Rev. B 40 (1989) 10481.
[23] J.E. Northrup, S. Froyen, Phys. Rev. Lett. 71 (1993) 2276.
[24] D.J. Chadi, J. Vac. Sci. Technol. A 5 (1987) 834.
[25] G.X. Qian, R.M. Martin, D.J. Chadi, Phys. Rev. B. 38 (1988) 7649.
[26] J.M. Holender, C. Jedrzejek, Surf. Sci. 247 (1990) 222.
[27] J. Falta, R.M. Tromp, M. Copel, G.D. Pettit, P.D. Kirchner, Phys. Rev. Lett. 69 (1992) 3068.
[28] I. Kamiya, D.E. Aspnes, D.E. Florez, D.E. Harbison, Phys. Rev. B 46 (1992) 15894.
[29] M. Sauvage-Simkin, R. Pinchaux, J. Massies, P. Calveric, N. Jedrecy, J. Bonnet, I.K. Robinson, Phys. Rev. Lett. 62 (1989) 563.
[30] P. Drathen, W. Ranke, K. Jacobi, Surf. Sci. 77 (1978) L162.
[31] M.D. Pashley, K.W. Haberern, J.M. Woodall, J. Vac. Sci. Technol. B 6 (1988) 1468.
[32] M.D. Pashley, K.W. Haberern, J.M. Gaines, J. Vac. Sci. Technol. B 9 (1991) 938.
[33] M.D. Pashley, K.W. Haberern, R.M. Feenstra, J. Vac. Sci. Technol. B 10 (1992) 1874.
[34] D.K. Biegelsen, R.D. Bringans, J.E. Northrup, L.E. Swartz, Phys. Rev. B 41 (1990) 5701.

[35] T. Hashizume, Q.K. Xue, J. Zhou, A. Ichimiya, T. Sakurai, Phys. Rev. Lett. 73 (1994) 2208.
[36] R. Duszak, C.J. Palmstrom, L.T. Florez, Y. Yang, J.H. Weaver, J. Vac. Sci. Technol. B 10 (1992) 1891.
[37] I. Karpov, N. Venkateswaran, G. Bratina, W. Gladfelter, A. Franciosi, J. Vac. Sci. Technol. B 13 (1995) 2041.
[38] V. Bressler-Hill, M. Wassermeier, K. Pond, R. Malboudian, G.A.D. Briggs, P.M. Petroff, W.H. Weinberg, J. Vac. Sci. Technol. B 10 (1992) 1881.
[39] J. Cerda, F.J. Palomares, F. Soria, Phys. Rev. Lett. 75 (1995) 665.
[40] S.L. Skala, J.S. Hubacek, J.R. Tucker, J.W. Lyding, S.T. Chou, K.Y. Cheng, Phys. Rev. B 48 (1993) 9138.
[41] M.A. Rueter, J.M. Vohs, Surf. Sci. 268 (1992) 217.
[42] W.T. Petrie, J.M. Vohs, Surf. Sci. 245 (1991) 315.
[43] A. Ludviksson, M. Xu, R. Martin, Surf. Sci. 277 (1992) 282.
[44] Royal Society Staff, Eight Peak Index of Mass Spectra, vol. 2., 3rd ed., The Mass Spectrometry Data Centre, The Royal Society of Chemistry, The University of Nottingham, UK, 1983.
[45] P.A. Redhead, Vacuum 12 (1962) 203.
[46] M.A. Rueter, J.M. Vohs, J. Vac. Sci. Technol. B 10 (1992) 2163.
[47] G.A. Domrachev, B.V. Zhuk, N.K. Zinovijeva, V.G. Kuleshov, I.V. Lomakova, Y.N. Krasnov, Inorg. Chim. Acta. 45 (1980) L233.
[48] H.D. Kaesz, F.G. Stone, Spectrochimica Acta. 15 (1959) 360.
[49] K. Nakamoto, Infrared and Raman Spectra of Inorganic and Coordination Compounds, 2nd ed., Wiley, New York, 1970.
[50] N. Venkateswaran, C.L. Roe, H.T. Lam, J.M. Vohs, Surf. Sci. 365 (1996) 125.
[51] E.I. Ko, J.B. Benziger, R.J. Madix, J. Catal. 62 (1980) 264.
[52] J.M. Heitzinger, J.G. Ekerdt, J. Vac. Sci. Technol. A 13 (1995) 2772.